Optical Anisotropy and Conformation of Macromolecules with Laterally Attached Mesogenic Side Groups

Peter N. Lavrenko*

Institute of Macromolecular Compounds, Russian Academy of Sciences, Bolshoi pr., 31, 199004 St. Petersburg, Russia

Igor P. Kolomietz

Institute of Physics, State University of St. Petersburg, Petrodvoretz, 198904 St. Petersburg, Russia

Heino Finkelmann

Institut für Makromolekulare Chemie, Universität Freiburg, Stefan-Meier-Strasse 31, 7800 Freiburg, FRG

*Received April 1, 1993; Revised Manuscript Received August 24, 1993**

ABSTRACT: Hydrodynamic, dynamooptic, and electrooptic properties have been investigated in dilute solutions of a methacryloyl polymer with the mesogenic cores laterally attached to side groups. Dependences of hydrodynamic properties on molecular weight varying from 5.7×10^5 to 3.0×10^6 and excluded volume effects are discussed. Unperturbed dimensions of the macromolecule are characterized by the Kuhn segment length $A = 70 \pm 10$ Å and by the steric factor $\sigma = 4.2$. From flow and electric birefringence measurements in a dilute solution, as well as in the liquid-crystalline phase, a shear optical coefficient and a specific Kerr constant for a polymer in solution were obtained. The optical anisotropy of the statistical segment and the mesogen were determined to be $\Delta\alpha_s = -(220 \pm 30) \times 10^{-25}$ cm^3 and $\Delta b = 230 \times 10^{-25}$ cm^3, respectively. The projection of a monomer dipole on the chain contour is $\mu_{0_l} = 0.4$ D. The orientational order parameter for the mesogenic cores in the isolated macromolecule was shown to be close to zero.

Introduction

Macromolecules with laterally attached mesogenic side groups possess a unique ability to form thermotropic liquid crystals with a biaxial nematic phase.[1] The properties of comb-shaped liquid-crystalline polymers with the rigid mesogenic groups attached to the backbone by its end (*end*-on polymer) either directly or via a spacer are known[2] to be strongly affected by the mesogen structure, the main chain flexibility, and the length and structure of the flexible spacer (chain part between the backbone and the mesogenic group). The influence of the type of attachment of the mesogenic group to the backbone on the properties of the concentrated solutions was investigated in few papers.[3] In this study, apparently for the first time, the properties of the isolated macromolecules with lateral structures are investigated as a function of molecular weight.

The insertion of side substituents into the monomer units of the macromolecule leads to a decrease in thermodynamic flexibility of the macromolecule owing to hindrance to rotation about valence bonds of the main chain, which is mainly caused by steric interactions. The equilibrium rigidity of the backbone of a comb-shaped macromolecule increases with side chain length.[4,5] For example, a degree of coiling of poly(alkyl acrylate) and poly(alkyl methacrylate) molecules with 16–18 carbon atoms in the alkyl moiety of the side chain, is about 3 or 4 times lower than that of typical flexible-chain polymers. For these polymers, the Kuhn segment length increases to 50–70 Å.

Investigations of birefringence in polymer solution in a flow (FB) and electric field (EB) have shown[6] that shear optical coefficient in solution of an *end*-on polymer with mesogenic side chains does not virtually depend on molecular weight and has the same sign as the Kerr constant. The optical anisotropy of the macromolecule being negative in sign essentially decreases in absolute value with insertion of an aliphatic spacer between the anisotropic mesogen group and the backbone. All this is true for the molecules with a long mesogenic group attached to the backbone by its end.

In this study, hydrodynamic, dynamooptic, and electrooptic investigations are made on a polymer, PMA, with symmetric three-ring mesogenic groups attached to the polymer backbone by its central ring via aliphatic spacer $-(CH_2)_{11}-$ (*side*-on polymer as designated in ref 7). This lateral type of the attachment of a mesogen is a fundamental difference between the structure of the PMA molecule and that of other comb-shaped liquid-crystalline *end*-on polymers investigated earlier.

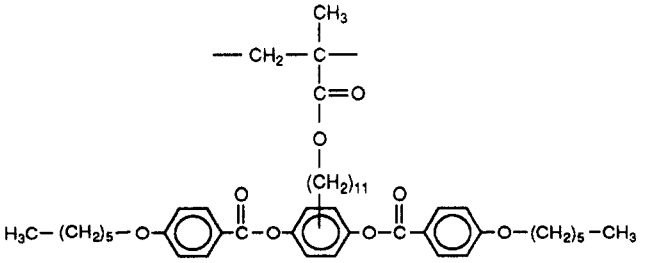

PMA

Experimental Section

The PMA samples were obtained by a published method.[1] According to gel permeation chromatography (GPC) with the data obtained in toluene with PS standards, the PMA samples have a wide molecular weight distribution (MWD), with indices listed in Table I.

Viscometry, sedimentation velocity, and free diffusion were investigated in benzene ("UV" grade) with density and viscosity of $\rho_0 = 0.8724$ g/mL and $\eta_0 = 0.583$ cP at 26 °C, respectively, and a refractive index of $n_D = 1.5011$. Flow birefringence (FB) and

* Abstract published in *Advance ACS Abstracts*, October 15, 1993.

0024-9297/93/2226-6800$04.00/0

Table I. Molecular Parameters for PMA Samples from Sedimentation Velocity and GPC Data

	IV sedim	IV GPC	III GPC	I GPC	II GPC
$M_w \times 10^{-6}$	6.8	1.19	1.257	0.68	0.49
M_w/M_n	3.8	2.73	3.22	5.77	4.51
M_z/M_w	2.1	2.28	2.02	3.52	3.01

the Kerr effect (EB) were investigated in carbon tetrachloride (CTC) with $\rho_0 = 1.5954$ g/mL, $\eta_0 = 0.96$ cP, and $n_D = 1.4607$ at 21 °C.

The viscosity of PMA solutions was measured in a capillary Ostwald viscometer with an average rate gradient of $g = 100\ s^{-1}$. For all dilutions, the flow time was above 60 s, and the kinetic energy correction was negligible. Intrinsic viscosity $[\eta]$ was obtained by extrapolating $[\eta] = \lim_{c\to 0} \eta_{sp}/c$ according to Huggins' equation $\eta_{sp}/c = [\eta] + [\eta]^2 k_H c$. The average value of Huggins' constant for PMA samples was $k_H = 0.40 \pm 0.07$.

Sedimentation velocity of PMA in benzene at 26 °C was investigated with an analytical ultracentrifuge (Model MOM-3180, Hungary) in a one-sector cell 1.2 cm thick at a rotation frequency of $n = 40 \times 10^3$ rpm. The accuracy of n was not lower than 0.2%. Fluctuations in temperature did not exceed ±0.05 K. The subsequent change in the form of concentration gradient distribution was recorded by a highly sensitive polarizing-interferometric optical means,[6] with spar twinning of 0.020 cm. Sedimentation coefficient was calculated from the time dependence of the first moment of the sedimentation curve, with subsequent extrapolation to zero concentration. The MWD for PMA sample IV and indices of its heterogeneity were determined from the time change in sedimentation curve spreading, with correction on the concentration effects.

Partial specific volume $\bar{v}$ for PMA in benzene was determined by the volume method. The densities of solutions with concentration c measured at 26 °C are given below: c (g/mL) 0.9215, 1.9641, 2.6072, 2.9574, 3.3971; ρ (g/mL) 0.8743, 0.8765, 0.8781, 0.8785, 0.8797. The dependence of ρ on c was linear. Hence, the expression $\rho = \rho_0 + (1 - \bar{v}\rho_0)c$ was used to calculate $\bar{v}$ which was found to be 0.903 mL/g.

Translational diffusion was investigated at 26 °C with a gradient method in which a sharp boundary was formed in a cell 3.0 cm thick in Tsvetkov's polarizing diffusometer.[6] Mutual diffusion coefficient D was evaluated by the height–area method. The time dependence of diffusion boundary spreading is shown in Figure 1a. The low concentrations of the solute (from 0.13 to 0.23 g/dL) made it possible to assume that the measured diffusion coefficient $(D_A)_c$ is close to the limiting D_A value, $D_A = \lim_{c\to 0} (D_A)_c$. This assumption is confirmed by the data in ref 7 which show that the maximum correction of D on the concentration effect at the c values used is not higher than 6%; i.e. it is within experimental error.

The refractive index increment was determined from the area under the diffusion curve. For PMA samples in benzene it was found to be $(dn/dc)_{546} = 0.044 \pm 0.001$ mL/g.

FB was investigated at 21 °C in a dynamooptimeter with an internal rotor[6] 3.0 cm in height with a gap of 0.03 cm. EB was measured at 20 °C in a rectangular pulsed electric field. A glass cell soldered in titanium electrodes 4.0 cm in length along the light beam path with a gap of 0.03 cm was used as the Kerr cell. The compensation method with a modulator[6,8] of polarized light ellipticity was used in both FB and EB measurements. The elliptical compensator had the optical retardations of 0.036λ (FB) and 0.01λ (EB) at wavelength λ. A He–Ne laser was used as a light source (λ = 632.8 nm). Birefringence measurements in the liquid-crystalline (LC) phase of PMA were performed with a MIN-8 polarizing microscope (USSR).

Results and Discussion

Hydrodynamic Properties. In sedimentation behavior of PMA in benzene, noticeable pressure effects were observed, when the sedimentation velocity was measured at different rotation frequencies n, from 22×10^3 to 60×10^3 rpm. Within experimental error, the time dependence of the first moment of the sedimentation curve in semilogarithmic coordinates (Figure 2) could be reliably

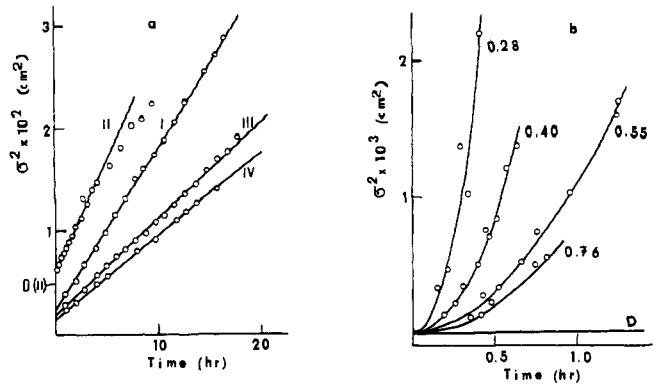

Figure 1. Time dependence of dispersion (second central moment) of the x-spectrum of the macromolecules in the region of diffusion (a) and sedimentation (b) boundaries in benzene solutions of PMA: a, for samples I, II, III, and IV; b, for sample IV at four concentrations indicated (in g/dL); curve D, diffusional dispersion calculated from $\sigma^2 = 2Dt$.

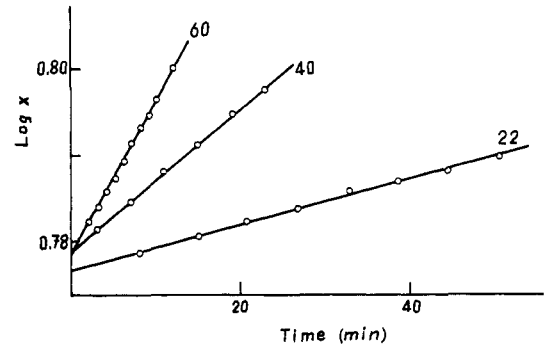

Figure 2. Time dependence of sedimentation boundary shift in a benzene solution of PMA sample IV (26 °C, $c = 0.28$ g/dL) at rotor rotation frequencies $n \times 10^{-3} = 60$, 40, and 22 rpm. The ordinate intercept values are equal to $\log x_0$ where x_0 is the abscissa of the meniscus.

approximated by linear functions. Effective values of the sedimentation coefficients s^p at a pressure p were calculated from the slopes of these dependences. The difference in s^p values obtained at different n, i.e. at different p, was found to be well approximated by relation $s^p = s(1 - \mu p)$. Here s is the s^p value at atmospheric pressure $p = 1$ and μ is a parameter of solvent compressibility. The μ value was obtained to be 2×10^{-9} cm s^2/g. This is close to the value known for benzene.[9] The exclusion of the pressure effects was performed by using the relation above and the sedimentation data obtained at $n = 40 \times 10^3$ rpm.

The concentration dependence $s(c)$ for PMA in benzene at low c is shown in Figure 3a. This corresponds to relation $1/s = (1/s_0)(1 + k_s c)$. The s_0 and k_s values obtained are listed in Table II. The average $k_s/[\eta]$ ratio was found to be 1.7 ± 0.1, which is close to that of a coiled macromolecule in a thermodynamically good solvent.[10]

The hydrodynamic data given in Table II and the value of $1 - \bar{v}\rho_0 = 0.211$ were used to determine the hydrodynamic invariant A_0 by[11]

$$A_0 = (D\eta_0/T)^{2/3}([\eta][s]R/100)^{1/3}$$

Here $[s] \equiv s_0\eta_0/(1 - \bar{v}\rho_0)$, R is the gas constant, and T the temperature. The average experimental A_0 value for PMA in benzene was found to be $(A_0)_{av} = (3.40 \pm 0.03) \times 10^{-10}$ erg/(K mol$^{1/3}$), and close to that of the other side-chain macromolecules.[11]

Molecular weight was determined from Svedberg's equation $M_{sD} = (RT/(1 - \bar{v}\rho_0))s_0/D$ using the s_0 and D_A values. With these M values, the molecular weight dependences of hydrodynamic properties for PMA samples

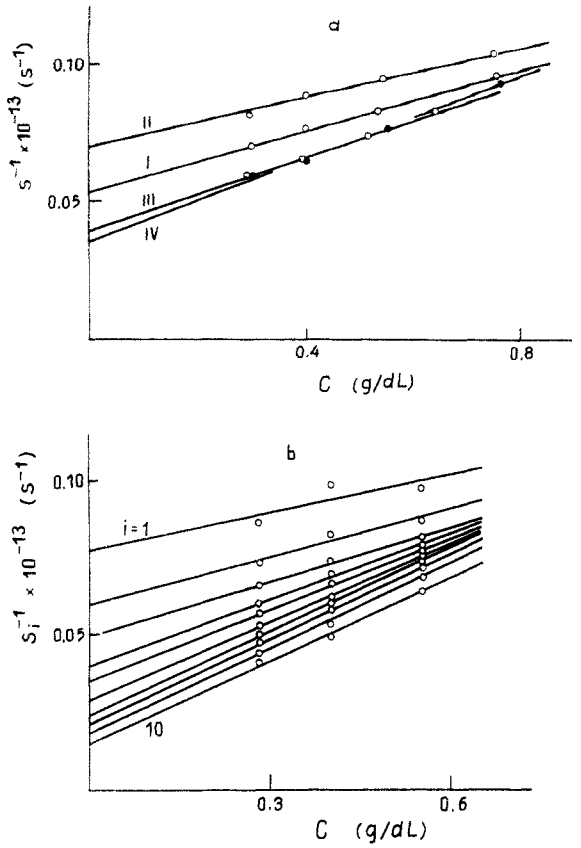

Figure 3. Concentration dependence of $1/s$ in benzene at n = 40×10^3 rpm for PMA samples (a) and for "graphic fractions" of PMA sample IV (b), where "i" denotes the number of fractions from the meniscus.

in benzene were established. A linear least-squares approximation of these dependences on a logarithmic scale (Figure 4) yields the following Mark–Kuhn–Houwink equations:

$$[\eta] = (1.25 \times 10^{-3})M^{(0.77\pm0.06)} \quad (\mathrm{cm}^3/\mathrm{g}) \quad (r = 0.994)$$

$$D_A = (8.0 \times 10^5)M^{-(0.60\pm0.01)} \quad (\mathrm{cm}^2/\mathrm{s}) \quad (r = 0.999)$$

$$s_0 = (6.8 \times 10^{-15})M^{(.40\pm0.01)} \quad (\mathrm{s}) \quad (r = 0.999)$$

Here r is the linear correlation coefficient. Taking into account the few samples and their significant polydispersity, these numerical coefficients should be considered as tentative values. Nevertheless, independent Burchard data[7] obtained for PMA (point 4 in Figure 4) are in quantitative agreement with the dependence $D(M)$ determined above.

Sedimentation Analysis of the PMA Samples Polydispersity. The sedimenting boundary in a benzene solution of PMA spreads rapidly with time, the spreading rate depending strongly on the solute concentration. The sedimentation boundary width was described by the dispersion of the *x-spectrum* defined by $\sigma^2 = \overline{x^2} - (\bar{x})^2$. The σ^2 is known to change with time in accordance with[12]

$$\sigma^2 = 2Dt + x^2\omega^4\sigma_s^2t^2 \quad (1)$$

Here $\omega = 2\pi n/60$ being the angular velocity of rotor rotation, and σ_s^2 the dispersion of the s-spectrum. The time dependence of σ^2 for solutions of PMA sample IV with concentrations from 0.28 to 0.76 g/dL (Figure 1b) clearly shows that in contrast to strong concentration effects, the contribution of diffusion spreading (curve D, first term in eq 1) to σ^2 is negligible.

Exclusion of the concentration effects was thus made by the point-by-point extrapolation method.[13] The x-spectrum was first transformed into the s-spectrum in an integral form and was then separated on the ordinate into 10 "graphic fractions" with subsequent extrapolation of sedimentation coefficient for each fraction s_i to vanishing concentration. The dependences of $1/s_i$ on c for the data of three experiments carried out for three different dilutions, from 0.28 to 0.55 g/dL, are shown in Figure 3b (the PMA solutions with lower concentrations were unavailable for investigations because of low refractive index increment). Assuming the linear approximation for each fraction, the values of $(1/s_i)_0 = \lim_{c\to0}(1/s_i)$ were obtained and, subsequently, transformed into M values using the M–K–H equation above. The MWD curve in Figure 5 was obtained in this manner for PMA sample IV. The indices of its heterogeneity are given in Table I.

Table I shows that all PMA samples are of significant polydispersity (Schulz' parameter is about 3). This is the reason for both the rapid spreading of the sedimentation boundary (clearly seen in Figure 1b) and a noticeable decrease in area under the diffusion curve which leads to experimental points falling lower than the linear dependence (e.g., curve II in Figure 1a) at long times. It can also be seen from Table I that the GPC data correctly reflect the relative values of molecular weight and index of polydispersity. In turn, the absolute value of the sedimentation-based M_w value differs from that obtained by GPC. This is the ordinary result for the newly engineered macromolecules because the M value is known to have only relative quantity when it is obtained by GPC with calibration by polymer standards of different structure.[14]

Conformational Parameters. As the exponents in the M–K–H equations differ from 0.5, and character of the concentration dependence $s(c)$ is as determined above, these factors show that excluded volume effects in the PMA–benzene system are considerable. This conclusion is also confirmed by the positive sign of the temperature coefficient for intrinsic viscosity. It was evaluated for PMA sample IV in benzene at temperatures varying between 18 and 73 °C to be $\Delta \ln[\eta]/\Delta T = +0.0041\ \mathrm{K}^{-1}$.

Therefore, the unperturbed dimensions of the isolated macromolecule and the characteristics of the equilibrium flexibility of the PMA chains were determined by extrapolating hydrodynamic data to the low M region where volume effects are absent. Burchard's plot of $[\eta]/M^{1/2}$ on $M^{1/2}$, described by the equation below,[15,16] was used.

$$[\eta]/M^{1/2} = K_\theta + 0.51\Phi_0 B\, M^{1/2} \quad (2)$$

Here $K_\theta = \Phi_0 M_L^{-3/2}A^{3/2}$, Φ_0 is the Flory coefficient for polymer coil in the theta solvent, M_L the mass per unit length, and B the parameter of thermodynamic interactions. The M_L value was taken to be the ratio of the monomer unit mass M_0 to its projection on the axis of the macromolecule λ: $M_L = M_0/\lambda$.

For PMA in benzene, a least-squares method yields the following linear approximation of the data

$$[\eta]/M^{1/2} = (2.52 \pm 0.62) \times 10^{-2} + [(2.94 \pm 0.46) \times 10^{-5}]M^{1/2} \quad (r = 0.976)$$

As follows from eq 2, the intercept K_θ gives the product $A\lambda$ and, hence, the statistical Kuhn segment length A. The application of $\Phi_0 = 2.86 \times 10^{23}\ \mathrm{mol}^{-1}$ (ref 17), $\lambda = 2.5$ Å (which follows from the PMA structure), and M_L = 302.4 $\mathrm{Å}^{-1}$ yields $A_\eta = 60 \pm 10$ Å.

A similar treatment of the sedimentation data was made by a plot of $M^{1/2}/s_0$ on $M^{1/2}$ described by the equation[18]

Table II. Hydrodynamic Properties of PMA Samples in Benzene at 26 °C

sample no.	$[\eta]$, dL/g	$10^{13}s_0$, s	k_s, mL/g	10^7D, cm^2/s	dn/dc, mL/g	$10^{-6}M_{sD}$, g/mol	$10^{10}A_0$, erg K^{-1} mol$^{-1/3}$
IV	1.35	28.2	210	1.10	0.045	3.02	3.43
III	1.09	25.6	170	1.26	0.042	2.39	3.38
I	0.51	18.5	100	2.16	0.044	1.01	3.37
II	0.38	14.2	62	2.95	0.045	0.57	3.45

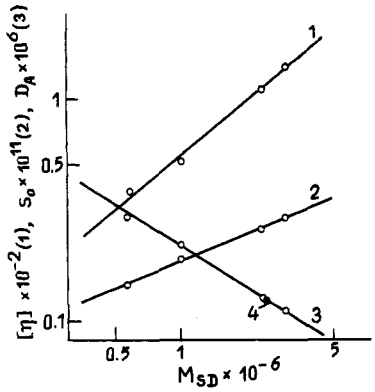

Figure 4. Dependence of $[\eta]$, s_0, and D_A on M_{sD} on a logarithmic scale for PMA in benzene at 26 °C: point 4, result from dynamic light scattering[7] of PMA in toluene when different viscosities of the solvents are taken into account.

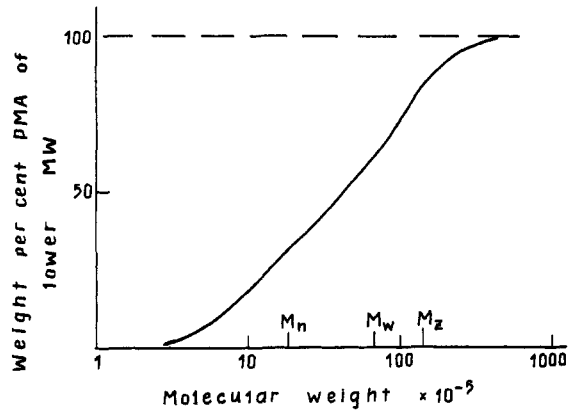

Figure 5. Integral molecular weight distribution for PMA sample IV obtained from sedimentation velocity data.

$$M^{1/2}/[s] = P_0N_AM_L^{-1/2}A^{1/2} + 0.2B_1P_0N_AM^{1/2} \quad (3)$$

with $B_1 = BM_L/A$ and Avogadro's number N_A. The least-squares method yields

$$M^{1/2}/s_0 = (4.56 \pm 0.10) \times 10^{-12} + [(9.30 \pm 0.78) \times 10^{-16}]M^{1/2} \quad (r = 0.993)$$

The application of $P_0 = 5.2$ (ref 18) in eq 3 yields $A_f = 81 \pm 5$ Å.

Besides eqs 2 and 3 there are some other plots which are expected to be linear dependences within a wider range of excluded volume effects.[19,20] However, a treatment of the experimental data by plotting, e.g., $([\eta]/M^{1/2})^{5/3}$, $(M^{1/2}/s_0)^5$, and $(M^{1/2}/s_0)^3$ versus $M^{1/2}$ was followed by decreasing r values, i.e. by loss in linearity of the approximations used and, hence, in reliability of the data extrapolation to $M = 0$.

It can be seen that the A_f value obtained from the translational friction data is higher than A_η determined from viscometric data. This result was also observed for other polymethacryloyl derivatives.[6] Partly, this difference may be due to inhomogeneity of the PMA samples. According to eqs 11 and 13 in ref 21, for heterogeneous samples, when the weight average M_w value is used as M, the first term in eq 2 is not K_θ but $K_\theta q_\eta$, and $P_0N_AM_L^{-1/2}A^{1/2}q_f$ in eq 3. Polymolecularity correction factors q_η and q_f for PMA were evaluated from Tables 8.1 and 9.1 given in ref 21 to be 0.90 and 1.06, respectively. Hence, this correction leads to A_η and A_f values close to 67 and 76 Å, respectively. We obtain that the heterogeneity effect can only decrease the difference between A_η and A_f from 30% to 13%.

A more serious reason for this difference is the fact that the theories used for the calculations of A_η and A_f are inadequate. This is manifested in mutual incompatibility[11] between the theoretical values of $P_0 = 5.2$ and $\Phi_0 = 2.86 \times 10^{23}$ mol^{-1}. These P_0 and Φ_0 values correspond to the value of $A_0 \equiv k_B(\Phi/100)^{1/3}/P = 3.77 \times 10^{-10}$ erg K^{-1} mol$^{-1/3}$ (with k_B the Boltzmann constant), whereas the experimental A_0 value is much lower, 3.4×10^{-10} erg K^{-1} mol$^{-1/3}$. In the coil limit, the theoretical Φ_0 value above seems to be overestimated whereas P_0 is underestimated.[22] Therefore, the $A = 70 \pm 10$ Å was taken as the average value.

The steric factor was calculated by $\sigma = (A/A_{free})^{1/2}$ to be 4.2 ± 0.6. Here A_{free} is the A value for the freely rotating chain. This σ value shows that the steric interactions of the side groups in the PMA chain in dilute solution strongly prevent the intramolecular rotation about the valence bonds in the main chain and lead to decreasing the equilibrium flexibility of the macromolecule by 3–4 times.

The comparison of this result with that of other polymethacryloyl derivatives[6] shows that the type of attachment the three-ring mesogenic group (by end point, or by the center point) as a side chain to the monomer units of the macromolecule does not influence markedly the equilibrium flexibility of an isolated macromolecule. It might be expected that this conclusion is valid only if there is a sufficiently long spacer (like in the PMA chain) between the backbone and the mesogenic group, which weakens the correlation in orientations of both the mesogenic group to the main chain and different mesogenic groups between each others.

The σ value 4.2 is also close to that obtained[23] in a benzene solution for side-chain polymer PTMA with the structure shown below. PTMA is not a mesomorphic

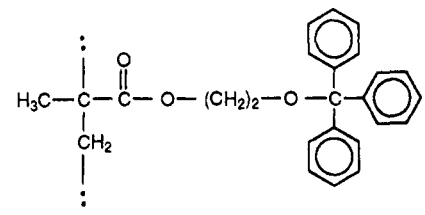

PTMA

polymer. Hence, high σ obtained for PMA is not a result of specific interactions between the side mesogen cores in the PMA chain but (as for PTMA) is due to steric interactions of bulky side groups.

The diameter of the PMA chain was estimated by using a model of a wormlike cylinder (with diameter d) which is completely and homogeneously filled by the polymer substance without solvent. Mass per unit cylinder length should, hence, be equal to the M_L for PMA, and d is simply related[24] to M_L: $d = (4\bar{v}M_L/\pi N_A)^{1/2}$. We obtain $d = 24$ Å. This value agrees qualitatively with the structure of the

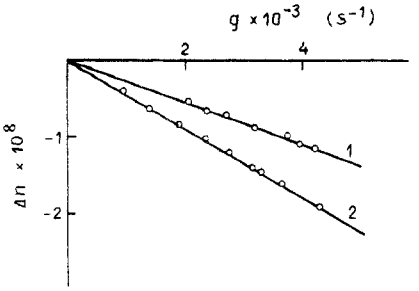

Figure 6. Shear rate (g) dependence of flow birefringence Δn in PMA solutions in CTC: curve 1, sample IV, c = 0.134 g/dL; curve 2, sample I, c = 0.384 g/dL.

PMA monomer unit and may be considered as a low (if we take into account the solvent effect) limit value for an effective hydrodynamic diameter of the PMA molecule in benzene solution.

Excluded Volume Effects. The expansion coefficient α for the PMA coils in benzene was evaluated from viscometric data by $\alpha = (\overline{r^2}/\overline{r_0^2})^{1/2} = ([\eta]\Phi_0/K_\theta\Phi M^{1/2})^{1/3}$ with the method of successive approaches for the Φ calculation using the $\Phi(\alpha)$ dependence given in ref 25. Here r and r_0 are end-to-end distances for the PMA molecule in benzene and under the theta conditions, respectively. The coefficient α was found to increase with M from 1.4 to 1.7 for the samples investigated. Thus, the hydrodynamic properties of PMA in benzene correspond to those typical of strongly expanded nondraining coils, with the number of segments in the chain from 27 to 140. The form asymmetry of the segment A/d does not exceed the value 2.9, and the volume part of a polymer substance ($M\bar{v}/N_A$) is not higher than 2% of the volume occupied by the PMA molecule coil in solution [$0.36(AM/M_L)^{3/2}\alpha^3$] (e.g. ref 6).

These PMA properties were compared with data for a comb-shaped *end*-on polymer PH with similar three-ring mesogenic groups fixed (without a spacer) to the ester groups of the main chain.

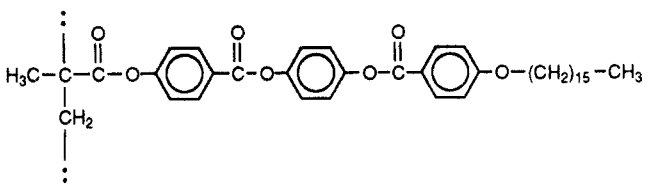

PH

According to ref 26, benzene is a theta solvent for PH, in contrast to its very good thermodynamical quality for PMA. The positions of aliphatic moieties of the side chains in the PH and PMA molecules (with respect to the main chain) are similar. Hence, a strong change (improvement) in the thermodynamic quality of benzene as solvent, on passing from PH to PMA, must be attributed to an increase in the orientational freedom of the three-ring mesogenic cores provided both by an introduction of the spacer and by another type of the mesogens attachment to the side chains of the macromolecule.

Dynamooptic Properties. Figure 6 shows the dependence of the FB Δn on the shear rate g for PMA samples I and IV in CTC. Experimental points were well approximated by a linear function with the slope giving the shear optical coefficient $\Delta n/\Delta\tau$

$$\Delta n/\Delta\tau = \Delta n/g(\eta - \eta_0)$$

where η is the solution viscosity.

Table III. Dynamooptic and Electrooptic Properties of PMA Samples in Carbon Tetrachloride at 21 °C

sample no.	$[\eta]$, dL/g	$10^{10}\Delta n/\Delta\tau$, cm s²/g	$10^{25}\Delta\alpha_s$, cm³	$10^{11}K$, cm⁵/g (300 V)²	μ_0, D[a]
IV	1.3	−15	−180	−(5.0 ± 0.3)	0.48
I		−20	−250	−(4.0 ± 0.3)	0.37

[a] 1 D = 1 × 10^{-18} CGSE units.

The $\Delta n/\Delta\tau$ values listed for PMA samples in Table III, were negative in sign, similar to those of other comb-shaped polymers having both aliphatic and mesogenic aromatic groups in the side chains.[6] The chains of the investigated PMA samples were shown above to have more than 27 Kuhn segments and, hence, to have the conformation of a random coil. For these chains, the shear optical coefficient does not depend on M and is determined by the optical anisotropy $\Delta\alpha_s$ of the Kuhn segment

$$\Delta n/\Delta\tau = (4\pi/45k_BT)[(n^2+2)^2/n]\Delta\alpha_s \quad (4)$$

Here n is the refractive index of the solvent. Substitution of n = 1.4607, T = 294 K and experimental $\Delta n/\Delta\tau$ values to eq 4 yields

$$\Delta\alpha_s = -(220 \pm 30) \times 10^{-25}\ \text{cm}^3$$

This $\Delta\alpha_s$ value characterizes the optical anisotropy of a segment of the PMA molecule in CTC. To determine the proper segment anisotropy, we must take into account the microform effect caused by the form asymmetry of the segment and the difference in refractive indexes of PMA and CTC. This effect was evaluated from[6]

$$\Delta\alpha_{fs} = (dn/dc)^2(M_0 s/\pi N_A \bar{v})\epsilon_s$$

with the form factor ϵ_s. Virtual coincidence in the $[\eta]$ values for PMA in benzene and CTC (Tables II and III) allows us to assume that s for PMA in CTC is close to s = 28 obtained above from hydrodynamic data on PMA in benzene. Substitution of dn/dc = 0.09 mL/g, M_0 = 756, $\bar{v}$ = 0.9 mL/g, s = 28, and ϵ_s = 0.297 (this value corresponds to segment axial ratio A/d = 2.5 (ref 6)) leads to $\Delta\alpha_{fs}$ = +300 × 10^{-25} cm³ for PMA in CTC. The proper optical anisotropy of the PMA chain segment is thus evaluated by

$$\Delta\alpha = \Delta\alpha_s - \Delta\alpha_{fs} = -(500 \pm 50) \times 10^{-25}\ \text{cm}^3$$

The $\Delta\alpha$ value is determined by both the optical anisotropy of atomic groups in a segment and the angle distribution of their axes with respect to the chain contour (direction of primary orientation of groups, i.e., the optical axis of the segment). The mesogenic groups contain the strongest anisotropic elements of the PMA structure. The contributions of the mesogenic groups to the optical anisotropy of the PMA molecule segment may be considered to be independent of each other because they are removed from the main chain by sufficiently long aliphatic spacers. Hence, we may represent $\Delta\alpha$ by the following sum

$$\Delta\alpha/s = \Delta b[(3\overline{\cos^2\theta} - 1)/2] + \Delta a \quad (5)$$

The first term here takes into account the optical anisotropy of the mesogenic group Δb and the angle θ formed by the optical axes of the group and the segment; $\overline{\cos^2\theta}$ is the value averaged over all mesogens. The second term in eq 5 is the optical anisotropy of the rest of the PMA monomer unit [methacryloyl and $-(CH_2)_{11}-$ groups]. The expression in brackets in eq 5 represents the orientational order parameter for the mesogenic groups

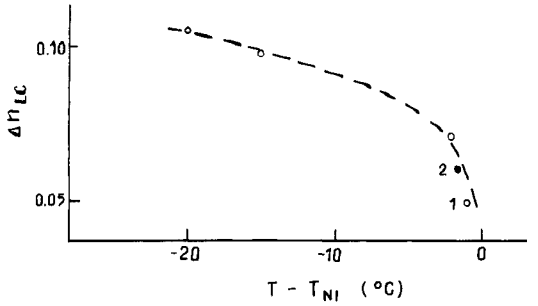

Figure 7. Temperature dependence of birefringence Δn_{mes} in the PMA LC phase, temperature counted from the transition point to the isotropic phase, $T_i = 60$ °C: point 1, sample 1; point 2, sample IV; solid curve, spline approximation of the experimental points.

$\overline{S_m} = (3\overline{\cos^2\theta} - 1)/2$ which may be evaluated from eq 5 when Δb and $\Delta\alpha$ are known.

Optical Anisotropy of the Mesogenic Group and the Segment. Birefringence Δn_{mes} in the PMA melt layer in the LC phase was investigated to determine the optical anisotropy of the mesogenic group Δb. A polymer layer between the planar and spherical surfaces of quartz glasses was employed. The planar orientation (director is parallel to the glass surface) in the layer was achieved by displacement of the upper glass. As a result of deformation, the pattern of concentric interference rings (curves of equal thickness) was observed with a polarizing microscope. The diameter of interference rings is related to Δn_{mes} by the equation[6]

$$\Delta n_{mes} = k\lambda/[R - (R^2 - d_k^2/4)^{1/2}] \quad (6)$$

Here $R = 2.606$ cm being the curvature radius of the spherical surface, $\lambda = 579$ nm being the wavelength, and d_k the diameter of a ring having number k. The diameters of several interference rings were measured, and Δn_{mes} was calculated according to eq 6.

Figure 7 shows the experimental results of birefringence measurements in the LC phase at different reduced temperatures. The T value was counted from the transition to the isotropic phase ($T_i = 60$ °C). The T-dependence of Δn_{mes} in Figure 7 is typical of nematic liquid crystals and reflects variation of the orientational order parameter S_{mes} with T. Δb was evaluated from[27]

$$\Delta n_{mes} = (4\pi/3)(\rho N_A/M_m)[(n^2 + 2)/2n]\,\Delta b\, S_{mes}$$

where ρ is the polymer density, n the mean refractive index of the liquid crystal, and M_m the mass of the mesogenic group. The Δb value was thus found to be $\Delta b = 230 \times 10^{-25}$ cm^3 if $\rho = 1$ g/mL, $n = 1.55$, and $S_{mes} = 0.6$ for $T - T_i = -10$ K were used. This Δb value is in good agreement with that of the nematic LC model compound A with a chemical structure similar to that of the mesogenic group in PMA.

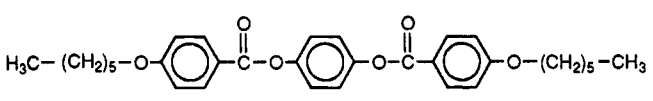

A

According to ref 28, the optical anisotropy of molecule A is equal to 210×10^{-25} cm^3, the dipole moment is 3 D, and the angle between the dipole direction and the optical axis of the molecule is 68°.

The anisotropy of polarizability of the mesogenic group may be characterized by $\delta = \Delta b/3\bar{\alpha}$ with an average polarizability of the group $\bar{\alpha}$ equal to $(\alpha + 2\beta)/3$. Here α and β are the main polarizabilities along the group axis and normal to it, respectively. The $\bar{\alpha}$ value was evaluated by the Lorentz–Lorenz expression

$$\bar{\alpha} = (3/4\pi)[(n^2 - 1)/(n^2 + 2)](M/\rho N_A)$$

Here M is the mass of molecule A and n the average value of refractive index for LC. The substitution of formula mass $M = 518$, $\Delta b = 230 \times 10^{-25}$ cm^3, $\rho = 1$, and $n = 1.5$ leads to $\bar{\alpha} = 6.0 \times 10^{-23}$ cm^3 and $\delta = 0.37$, respectively.

The average polarizability of the segment $\overline{\alpha_s}$ for PMA in CTC was obtained as polarizability of the macromolecule related to the number of segments

$$\overline{\alpha_s} = (n_0 M/2\pi N_A)(dn/dc)/(M/M_0 s)$$

The substitution of $M_0 = 756$, $n_0 = 1.4607$, $s = 28$, and $dn/dc = 0.09$ mL/g leads to $\overline{\alpha_s} = 7.4 \times 10^{-22}$ cm^3. The anisotropy of the segment polarizability defined by $\delta_s = \Delta\alpha/3\overline{\alpha_s}$ was thus found to be equal to 0.068. This is a few times less than that of the polarizability of the mesogenic group.

Orientational Order in Mesogenic Groups. The ordering of the mesogenic group optical axes is described by orientational order parameter S_m which may be evaluated from eq 5. To use eq 5, the optical anisotropy of the monomer units of poly(octyl methacrylate) -5.9×10^{-25} cm^3, and poly(cethyl methacrylate),[29] -8.9×10^{-25} cm^3 were chosen as the Δa value. The substitution of these Δa, and Δb and s values obtained above, into eq 5 yields the order parameter S_m close to zero, $S_m = 0.02 \pm 0.02$. This S_m value is acceptable only in two cases of distribution of the mesogenic group axes with respect to the main chain contour. In the first case, the orientational correlation between the mesogenic groups and the main chain is absent. In the second one, this correlation takes place but with symmetric distribution of projections of the mesogenic groups on the chain contour, the dispersion of which $\overline{\cos^2\theta}$ is close to 1/3 (hence, the average θ value is close to 55°).

Note that calculations made above are qualitative because the FB data may also be influenced by the macroform effect[6] caused by aspherical distribution of the polymer mass in a coiled macromolecule in a dilute solution where $dn/dc \neq 0$. This effect would, in principle, increase the S_m value up to −0.16 but does not change the main conclusions. On the other hand, the noticeable macroform effect should also lead to $\Delta n/\Delta\tau$ increasing with M in contrast to the experimental data in Table III. This shows that additional data must be applied to quantitative determination of the order parameter.

Electrooptic Properties. Figure 8 shows the dependence of EB Δn on the square field strength E^2 in solutions of PMA in CTC. The slope of straight line provides the Kerr constant for CTC $K_0 = \Delta n/E^2 = 5 \times 10^{-13}$ cm^5 g^{-1} (300 V)$^{-2}$, and specific Kerr constant for PMA by $K = (K_c - K_0)/c$, where K_c is the K value for a solution with concentration c. The results are given in Table III.

For PMA in CTC, the signs of the Kerr constant and the shear optical coefficient $\Delta n/\Delta\tau$ coincide as well as those of other LC side-chain polymers elsewhere investigated,[6,26] particularly, for PH and polymer B.

The Kerr constant for PMA coincides in the order of the magnitude with that[30] of polymer B with the mesogenic groups attached to the main chain via the aliphatic spacer of length similar to that in PMA. On the other hand, the Kerr constant value is about 2 orders lower than that of PH where the same mesogenic moiety (as in PMA) is attached directly to the main chain.[6] This result agrees

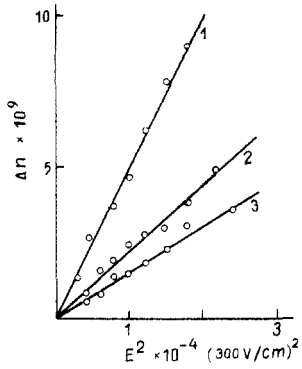

Figure 8. Electric birefringence Δn vs square electric field strength E^2 in CTC (1) and in solutions of the PMA samples (2, 3): curve 2, sample I, c = 0.75 g/dL; curve 3, sample IV, c = 0.64 g/dL.

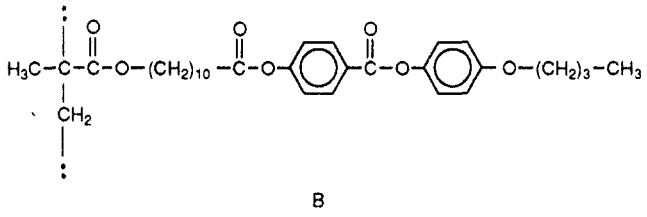

B

well with the concept that a long flexible spacer strongly lowers the correlation in the orientations of the mesogens in the side chains with respect to the main chain in the PMA macromolecule.

The coincidence in signs of K and $\Delta n/\Delta\tau$ may be attributed, as was suggested elsewhere,[6] to the existence of the longitudinal component $\mu_\parallel$ of the dipole moment of the macromolecule. It is the sum of tangential components of the monomer dipole moments $\mu_{0\parallel}$ which was evaluated from[6]

$$\mu_{0_\parallel} = \left[\frac{54k_BTM_0}{(\epsilon+2)^2N_As}\frac{K}{\Delta n/\Delta\tau}\right]^{1/2}$$

with ϵ = 2.238 being the dielectric permeability of CTC. For PMA, the obtained value $\mu_{0_\parallel}$ = 0.4 D is in the same range as the data of other methacryloyl *end*-on polymers with different mesogenic groups attached directly (or via an aliphatic spacer) to the main chain.[6]

Conclusion

The structure of the PMA molecule without mesogenic groups is close to that of the poly(cethyl methacrylate) molecule (PCMA). The Kerr constant for PCMA is equal to $K = 0.28 \times 10^{-11}$ cm^5 g^{-1} (300 V)$^{-2}$.[6] This not only is 1 order lower in absolute value than K for PMA but also has the opposite sign. This means that it is the mesogenic groups that determine the value and sign of the Kerr constant for PMA and, hence, the $\mu_{0_\parallel}$ value.

On the other hand, the presence, in the PMA chains, of the longitudinal dipole component provided by the mesogenic groups, is virtually impossible when orientational ordering of the mesogens in the direction of the chain contour is absent. In this case, the low (according to FB data) value of the orientational order parameter S_m should imply that the direction of the mesogenic group axes forms an angle (to the segment axis) with the average value close to 55°.

This interpretation does not exclude an alternative assuming the virtual absence of the orientational ordering of the mesogens with respect to the chain contour. This is confirmed by both the coincidence in signs and the relatively small difference in values (less than 2 times) of the Kerr constant for PMA and a mesogen model compound A: $K = -2.9 \times 10^{-11}$ cm^5 g^{-1} (300 V)$^{-2}$.[28] This similarity of the electrooptic properties of PMA and compound A may be interpreted as the virtual absence (in the EB phenomenon) of apparent linkage of the mesogens with the PMA main chain.

Thus, the analysis of the FB and EB data shows the correlation between dynamooptic and electrooptic investigations, indicative of the low value of the orientational order parameter for the mesogens with respect to the PMA main chain contour.

Hence, the lateral type of the mesogen groups attachment to the PMA side chain does not markedly influence the equilibrium flexibility of the macromolecule, but leads to high disordering in the space orientation of the mesogenic groups, more pronounced than that due to the increase in the flexible spacer length alone. This conclusion follows from the hydrodynamic properties discussed above, from increasing excluded volume effects and decreasing optical anisotropy and the dipole moment of the macromolecule. On the other hand, the formation of the LC phase, for the same reason, must proceed easier in the melt of the *side*-on polymer than in the *end*-on one.

Note, at last, that the values of anisotropy of segment polarizabilities, δ_s, and the number of monomer units in a Kuhn segment, s = 28 ± 4, obtained above, are in qualitative correlation with the data of Burchard et al.[3] on depolarization of light scattering. This accordance may be considered particularly satisfactory because the data in ref 3 were obtained in chloroform, whereas in this work CTC and benzene were used as solvents. At the same time, it is known that for LC side-chain polymers, conformational and optical properties of the macromolecules may be strongly affected by the nature of the solvent.[6,26]

Acknowledgment. The authors are much obliged to O. V. Okatova, A. V. Lezov, E. V. Korneeva, and A. M. Ovsipyan for the participation in the experimental part of the work. The GPC analysis was kindly performed by E. Stibal-Fisher.

References and Notes

(1) Hessel, F.; Herr, R.-P.; Finkelmann, H. *Makromol. Chem.* **1987**, *188* (7), 1597.
(2) Finkelmann, H.; Rehage, G. *Adv. Polym. Sci.* **1984**, *60/61*, 99.
(3) Richtering, W.; Gleim, W.; Burchard, W. *Macromolecules* **1992**, *25* (14), 3795.
(4) Andreeva, L. N.; Gorbunov, A. A.; Didenko, S. A.; Korneeva, E. V.; Lavrenko, P. N.; Plate, N. A.; Shibaev, V. P. *Vysokomol. Soedin.* **1973**, *15B* (3), 209.
(5) Ricker, M.; Schmidt, M. *Makromol. Chem.* **1991**, *192* (3), 679.
(6) Tsvetkov, V. N. *Rigid-Chain Polymers*; Plenum Publishing Corp.: New York, 1989.
(7) Richtering, W. H.; Schätzle, J.; Adams, J.; Burchard, W. *Colloid Polym. Sci.* **1989**, *267* (7), 568.
(8) Tsvetkov, V. N.; Kolomietz, I. P.; Lezov, A. V.; Stepchenkov, A. S. *Vysokomol. Soedin.* **1983**, *25A* (6), 1327.
(9) Elias, H.-G. *Makromol. Chem.* **1959**, *29B* (1/2), 30.
(10) Lavrenko, P. N.; Frenkel, S. Ya. *J. Polym. Mater.* **1991**, *8* (2), 89.
(11) Tsvetkov, V. N.; Lavrenko, P. N.; Bushin, S. V. *J. Polym. Sci., Polym. Chem. Ed.* **1984**, *22* (11), 3447.
(12) Baldwin, R. L.; Williams, J. W. *J. Am. Chem. Soc.* **1950**, *72* (9), 4325.
(13) Gralen, N.; Lagermalm, G. *J. Phys. Chem.* **1952**, *56* (4), 514.
(14) See, e.g.: Percec, V.; Tomazos, D.; Feiring, A. E. *Polymer* **1991**, *32* (10), 1897.
(15) Burchard, W. *Makromol. Chem.* **1961**, *50* (1), 20.
(16) Stockmayer, W. H.; Fixman, M. *J. Polym. Sci., Part C* **1963**, *1*, 137.
(17) Auer, P. L.; Gardner, C. S. *J. Chem. Phys.* **1955**, *23* (8), 1545.
(18) Cowie, J. M. G.; Bywater, S. *Polymer* **1965**, *6* (3), 197.

(19) Tsvetkov, V. N.; Hardy, D.; Shtennikova, I. N.; Korneeva, E. V.; Pirogova, G. F.; Nitray, K. *Vysokomol. Soedin.* **1969**, *11A* (2), 349.
(20) Tanaka, G. *Macromolecules* **1982**, *15* (4), 1028.
(21) Bareiss, R. E. In *Polymer Handbook*; Brandrup, J., Immergut, E. H., Eds.; Wiley-Interscience: New York, 1988; part VII, p 149.
(22) Yamada, T.; Yoshizaki, T.; Yamakawa, H. *Macromolecules* **1992**, *25* (1), 377.
(23) Lavrenko, P. N.; Pavlov, G. M.; Otoupalova, Ya.; Korneeva, E. V.; Polotsky, A. E. *Vysokomol. Soedin.* **1975**, *17A* (7), 1522.
(24) Bohdanecký, M. *Macromolecules* **1983**, *16* (9), 1483.
(25) Ptitsyn, O. B.; Eizner, Yu. E. *Vysokomol. Soedin.* **1959**, *1* (7), 966.
(26) Tsvetkov, V. N.; Shtennikova, I. N.; Kolbina, G. F.; Bushin, S. V.; Mashoshin, A. I.; Lavrenko, P. N.; Baturin, A. A.; Amerik, Yu. B. *Vysokomol. Soedin.* **1985**, *27A* (2), 319.
(27) De Jeu, W. H. *Physical Properties of Liquid Crystalline Materials*: Gordon A. Breach Sci. Publ.: New York, 1980.
(28) Ryumtsev, E. I.; Rotinyan, T. A.; Kovshik, A. P.; Agafonov, M. A. *Opt. Spektrosk.* **1985**, *51* (1), 131.
(29) Tsvetkov, V. N.; Andreeva, L. N. *Adv. Polym. Sci.* **1981**, *39*, 95.
(30) Pogodina, N. V.; Tsvetkov, V. N. *Vysokomol. Soedin.* **1982**, *24A* (11), 2275.